Published in final edited form as:
Nature. 2008 September 25; 455(7212): 542–546. doi:10.1038/nature07255.

FcRn-mediated antibody transport across epithelial cells revealed by electron tomography

Wanzhong He[1,2], **Mark S. Ladinsky**[3], **Kathryn E. Huey-Tubman**[1,4], **Grant J. Jensen**[1], **J. Richard McIntosh**[3], and **Pamela J. Björkman**[1,4]

[1]Division of Biology 114-96, California Institute of Technology, 1200 East California Blvd., Pasadena, CA 91125.

[2]Department of Biological Sciences, National University of Singapore, 14 Science Drive 4, Singapore 117543.

[3]Boulder Laboratory for 3D Electron Microscopy of Cells, Department of Molecular, Cellular and Developmental Biology, University of Colorado, Boulder, CO 80309.

[4]Howard Hughes Medical Institute, California Institute of Technology, 1200 East California Blvd., Pasadena, CA 91125.

Abstract

The neonatal Fc receptor (FcRn) transports maternal IgG across epithelial barriers[1,2], thereby providing the fetus or newborn with humoral immunity before its immune system is fully functional. In newborn rodents, FcRn transfers IgG from milk to blood by apical-to-basolateral transcytosis across intestinal epithelial cells. The pH difference between the apical (pH 6.0-6.5) and basolateral (pH 7.4) sides of intestinal epithelial cells facilitates efficient unidirectional transport of IgG, since FcRn binds IgG at pH 6.0-6.5 but not pH ≥7 [1,2]. As milk passes through the neonatal intestine, maternal IgG is removed by FcRn-expressing cells in the proximal small intestine (duodenum, jejunum); remaining proteins are absorbed and degraded by FcRn-negative cells in the distal small intestine (ileum)[3-6]. We used electron tomography to directly visualize jejunal transcytosis in space and time, developing new labeling and detection methods to map individual nanogold-labeled Fc within transport vesicles[7] and to simultaneously characterize these vesicles by immunolabeling. Combining electron tomography with a non-perturbing endocytic label allowed us to conclusively identify receptor-bound ligands, resolve interconnecting vesicles, determine if a vesicle was microtubule-associated, and accurately trace FcRn-mediated transport of IgG. Our results present a complex picture in which Fc moved through networks of entangled tubular and irregular vesicles, only some of which were microtubule-associated, as it migrated to the basolateral surface. New features of transcytosis were elucidated, including transport involving multivesicular body inner vesicles/tubules and exocytosis via clathrin-coated pits. Markers for early, late, and recycling

Author Information Reprints and permissions information is available at www.nature.com/reprints. The authors declare no competing financial interests. Correspondence should be addressed to P.J.B. (bjorkman@caltech.edu)..

Author Contributions W.H. and P.J.B. conceived the experiments. EM data were collected by W.H. in collaboration with and in the microscopy laboratory established by G.J.J. at Caltech. W.H. configured SerialEM on the Caltech electron microscopes, prepared intestinal samples by chemical fixation or HPF/FSF, conceived and developed the gold enhancement procedures, collected, processed, interpreted, and modeled tomograms. W.H. and K.E.H.T conducted kinetic experiments. Immunolabeling and associated imaging was done by M.S.L. in Boulder using enhanced samples provided by W.H. and K.E.H.T. Initial phases of the project using transfected cells were conducted by P.J.B. in Boulder in collaboration with J.R.M. and the Boulder Laboratory for 3D Microscopy of Cells. All authors discussed and interpreted the results and edited the manuscript.

Supplementary Information is linked to the online version of the paper at www.nature.com/nature.

Full Methods and any associated references are available in the online version of the paper at www.nature.com/nature.

endosomes each labeled vesicles in different and overlapping morphological classes, revealing unexpected spatial complexity in endo-lysosomal trafficking.

To prevent ligand misdirection caused by a bulky label, we covalently attached small (1.4nm) Nanogold to IgG-Fc (Au-Fc) at a site distant from where FcRn binds[7]. To avoid attaching >1 ligand/gold, which could artifactually prolong release through avidity, we used monofunctional Nanogold and purified Au-Fc by sizing and FcRn-affinity chromatography[7]. For steady-state experiments, Au-Fc was fed to neonatal rats, rather than incubated with excised intestines, which causes morphological changes[5]. The concentration of ingested Au-Fc was approximately equal to IgG in rat milk, because previously-used higher concentrations[5] saturated FcRn, resulting in degradation of excess IgG[8]. Intestinal samples were prepared for electron tomography by high pressure freezing, freeze-substitution fixation (HPF/FSF), the most accurate method for preserving dynamic trafficking events and ultrastructure[9], and we developed methods to enlarge endocytosed Nanogold during FSF[7,10].

Internal controls verified that enlarged gold accurately marked transported Au-Fc: (i) Gold was in physiologically-relevant locations (apical surface, tubulovesicular compartments in proximal cells; inside degradative compartments in distal cells), but not in nuclei, mitochondria, the ER or Golgi (Fig.1-5; Supplementary Fig.S1-S7); (ii) ≥98% of particles in proximal cells were 6-7nm from a membrane (Supplementary Table S1), consistent with Au-Fc bound to FcRn; and (iii) Au-Fc, but not Au-dextran, was enhanced in proximal (FcRn-positive) cells, whereas both were enhanced in distal (FcRn-negative) cells, reflecting receptor-mediated and fluid-phase uptake in the proximal and distal intestine, respectively (Fig.1a; Supplementary Fig.S7).

More than 50 tomograms, each ~1.8 μm^3, were recorded from jejunal cells from Au-Fc-fed neonatal rats (steady-state experiments) (Supplementary Table S1). For kinetic analysis, ligated intestinal lumens were incubated with Au-Fc (>50 pulse or pulse/chase tomograms or projections) (Supplementary Table S3). We defined three jejunal cell regions (Fig.1b): Region 1: microvilli and terminal web[11], Region 2: between the terminal web and nucleus, and Region 3: the lateral intercellular space (LIS) (basolateral membrane) and nearby cytoplasmic regions (Supplementary Fig.S4-S5). Region 3 was considered separately from Region 2 because vesicles near the LIS participate in exocytosis/endocytosis. Within these regions, we classified gold-containing features into categories (Supplementary Table S1, Fig.S8): clathrin-coated pits at the apical/basolateral membranes, regular ~60nm diameter tubular vesicles (RTVs – uniform diameters; variable lengths), coated buds/tips on RTVs, coated and uncoated spherical vesicles, irregular >70nm tubular vesicles (ITVs – variable diameters/lengths), irregular nontubular vesicles (INTVs), coated/uncoated bulbs in ITVs/INTVs, multivesicular bodies (MVBs), and MVB inner vesicles, protrusions, and tubules. Compartments that contained enlarged Au-Fc were further characterized by immunolabeling using antibodies against early (EEA1 and Rab5), late (Rab7 and Rab9), and recycling (Rab11) endosomes[12]. RTVs labeled with EEA1 and Rab5, MVBs with Rab5, and ITVs and INTVs with all five markers, although mainly Rab5, Rab9 and Rab11 (Fig. 1h-i; Supplementary Fig.S9, Table S2). These results demonstrated the morphological complexity of the endo-lysosomal system, revealing that "early", "late", and "recycling" endosomes, as defined by their expression of markers, do not represent single categories of vesicles.

In Region 1, we found Au-Fc on microvillar surfaces (suggesting receptor-mediated uptake at acidic pH), and in 60-120nm clathrin-coated pits (Fig.1c-g; Supplementary Fig.S8, Movie 1). Most Au-Fc endocytosis involved coated pits at the base of microvilli; many were proximal to gold-containing RTVs (Fig.1c,g, Supplementary Fig.S3,S4). Pulse experiments (Supplementary Table S3) suggested that the first transport steps involved a coated vesicle pinching off from a coated pit, uncoating, and fusing with a RTV or apical irregular vesicle.

In Region 2, Au-Fc was in RTVs, ITVs, INTVs, and MVBs. RTVs had nearly uniform diameters (Supplementary Fig.S8; Fig.1c,2a-b), but lengths between ~0.2-3.0μm, and could branch, bend and loop (Supplementary Fig. S3,S4, Movie 2). Gold-containing spherical coated vesicles (Fig.2c) were found throughout this region; their ~60nm diameter (Supplementary Fig.S8) suggested derivation from ~60nm coated tips/buds of RTVs (Fig.2d), as found for transferrin receptor/transferrin trafficking[13]. Irregularly-shaped vesicles, both non-tubular (INTVs) (Fig.3a-c) and tubular (ITVs) (Fig.2e,3d), also included gold. Similar to RTVs, Au-Fc reached ITVs and INTVs within 5-7min, but unlike RTVs, ITVs/INTVs were rarely in Region 1, suggesting they were populated after Region 1 RTVs. Some ITVs contained 70-130nm bulbs (Fig.3d) and/or small internal vesicles. INTVs included gold-containing 70-150nm bulbs (Fig.3c; Supplementary Movies 3-4). Coated bulbs on irregular vesicles were smaller (70-80nm) than most uncoated bulbs (70-150nm), but broader than the ~60nm coated buds on RTVs (Supplementary Fig.S8). ITVs were often intertwined with INTVs and MVBs, but not with RTVs (Fig.2f-h,3e; Supplementary Fig.S11, Movies 2-4). Some gold-containing tubular vesicles were aligned with microtubules (Fig. 2b,f; Supplementary Movies 2-4), suggesting microtubule-based motor movement, consistent with nocodazole disruption of FcRn-mediated transport[14].

Au-Fc appeared in Region 2 MVBs within 5min of uptake and throughout a 25min chase (Supplementary Table S3), always attached to a membrane (Fig.4 and Supplementary Movies 4,5), suggesting binding to FcRn. In contrast, in the ileum where IgG is degraded[5], gold was randomly distributed in MVB-like vesicles (Supplementary Fig.S2d-e). Jejunal MVBs appeared as predominantly Rab5-positive 0.3-1.2μm spherical vesicles, sometimes associated with microtubules, which contained small (40-90nm) inner vesicles (Fig.1h-i,4; Supplementary Fig.S8, Table 2). As observed in dendritic and B cells[15], jejunal MVB inner vesicles were detached, not invaginating tubules open to cytoplasm (Supplementary Movies 4-5). Au-Fc was associated with the inner surface of the main MVB membrane and the outer surfaces of inner vesicles. Fusion of a FcRn-Fc-containing vesicle with a MVB accounted for the former; formation of an inner vesicle from a gold-associated membrane accounted for the latter. Accordingly, we observed invaginations and protrusions in the main membranes of MVBs (Fig.4d).

Some jejunal MVBs contained 50-130nm diameter tubular protrusions (Supplementary Fig.S8), often resembling ITVs. Gold was found along the length and tips of these tubules, suggesting a reorganization of jejunal MVBs similar to that seen in dendritic cells when vesicles derived from MVB tubule tips carry class II MHC/peptide complexes to the cell surface[16]. A similar role for MVBs and their protrusions in Au-Fc transcytosis implies that MVBs serve primarily transport, not degradative, processes during FcRn-mediated transport across the intestine. In support, jejunal MVBs exhibited hallmarks of early endosomes: they contained relatively few internal vesicles[17] (Fig.4) and labeled with markers for early and recycling, but not late, endosomes (Fig.1h-i; Supplementary Table S2).

Region 3 was distinguished from Regions 1-2 by fewer tubular vesicles (Fig.5a), more irregular vesicles, and an abundance of clathrin (Supplementary Fig.11d, Movie 6). Apical to the nucleus, Au-Fc was in ITVs, INTVs, 70-140nm spherical vesicles, and coated pits within the LIS membrane. FcRn-mediated transcytosis of Au-Fc was demonstrated by extracellular gold in narrow regions and pockets of the LIS (Fig. 5a, Supplementary Movies 6-8) (accounting for ~10% of Au-Fc; Supplementary Table S1) and below the cell (Supplementary Fig.S1f,S6). The first Au-Fc reached the LIS ~10min after uptake, with most appearing after 15-30min (Supplementary Table S3). Extracellular Au-Fc and intracellular gold-containing vesicles were largely apical of the nucleus.

Clathrin was found coating gold-containing vesicles, bulbs and pits, and free in the cytosol (Supplementary Movies 6-7). In chemically-fixed samples, clathrin triskelions clearly formed the characteristic polygonal lattice (Supplementary Movie 6) containing mostly hexagons with occasional pentagons and heptagons (Fig.5b). If, as commonly assumed, clathrin coats are shed prior to vesicle fusion[18-21], gold-containing coated pits at the basolateral membrane would represent snapshots of endocytosis, which cannot normally be distinguished from exocytosis by EM. However, FcRn-mediated IgG transcytosis across the neonatal intestine represents one of the only systems in which receptor-mediated re-uptake of exocytosed ligands is strongly disfavored: the neutral/basic pH at the basolateral surface should not allow large-scale FcRn-mediated endocytosis of Au-Fc, which was present at a concentration that would not allow binding to FcRn at pH ≥ 7 (Supplementary Discussion). The simplest interpretation of the gold-containing coated pits at the LIS membrane is that most/all represent partially-uncoated vesicles undergoing exocytosis. In support, we found ≥100 gold-containing coated pits in the basolateral membrane (Supplementary Table S1), but saw no definitive examples of gold in an uncoated pit. Thus if these coated pits were not exocytosing, we did not observe any obvious exocytic events although released Au-Fc was in the extracellular space. Partially uncoated vesicles, which could accumulate during the slow, steady-state uncoating occurring after an initial burst of uncoating[22], might allow their uncoated portion to fuse with the basolateral membrane.

The existence of partially-fused and partially-coated vesicles is compatible with either “kiss and run”[23] or “prolonged release”[24] exocytosis, in which a transient pore opens to release the vesicle’s contents. However, FcRn-mediated exocytosis cannot completely conform to “kiss and run” release of small molecules from 0.3-3.5nm pores[25], because IgG and Fc dimensions approach 10nm. Accordingly, gold-containing clathrin-coated pits in the LIS membrane were 90-150nm, typically larger than their apical counterparts (60-120nm), where mainly endocytosis is expected (Fig.1,5; Supplementary Fig.S8).

As occurs in other exocytosis systems[26], clathrin-mediated endocytosis at the basolateral surface likely retrieves FcRn and the original vesicle after IgG release. Thus we propose that clathrin is maintained on membrane invaginations undergoing exocytosis to facilitate receptor recovery so FcRn can contribute to another round of apical-to-basolateral transcytosis. This may be a specialized adaptation of neonatal jejunal cells for their primary function – IgG transport[5]. Indeed, clathrin levels near the LIS were unusually high in neonatal jejunal cells (Supplementary Movie 6) , but become noticeably reduced after weaning[5]. Further studies will be required to definitively address whether partially uncoated vesicles can fuse, and if so, whether unique features (e.g., specialized machinery and/or low levels of vesicle uncoating enzymes) facilitate this type of fusion in neonatal jejunal cells.

Steady-state and kinetic experiments revealed parallel transport pathways as summarized in Fig.5h. In initial steps, Au-Fc enters jejunal cells in apical coated pits, and derived coated vesicles likely fuse, presumably after uncoating, with apical RTVs and/or with irregular vesicles. Coated buds on RTVs could serve as exit points, pinching off to shuttle Au-Fc to MVBs, ITVs, and INTVs in Regions 2-3. Au-Fc in clathrin-rich cytoplasmic regions near the LIS then transits through clathrin-coated spherical or irregular vesicles prior to exocytosis from a coated pit, which could be endocytosed to recycle FcRn. As a general feature, most potential transport vesicles contained a few Au-Fc instead of a seemingly more efficient system in which a specialized subset of vesicles containing many Au-Fc moved purposefully (e.g., along microtubule tracks) to the basolateral membrane. Rather, most gold-containing vesicles were not visibly associated with microtubules, and vesicle-associated microtubules were not arranged in any particular direction.

Vesicle morphologies and intracellular contexts were compatible with kinetic data. First, RTVs, early endosomes containing ~20% of Au-Fc (Supplementary Table S1), were mainly in Regions 1-2, and were not entangled with ITVs or INTVs. RTVs probably move FcRn-Fc complexes by microtubule-based travel or by releasing vesicles derived from ~60nm coated buds. Both ITVs and INTVs usually had larger (70-80nm) coated bulbs, as well as still larger uncoated bulbs, and these vesicles formed intertwined networks near the LIS with MVB tubules and each other (Fig.3e). ITVs and INTVs accounted for ~34% of Au-Fc (Supplementary Table S1), suggesting a major role for irregular vesicles in FcRn-mediated transcytosis. Morphological similarities suggested that MVB tubules were related to ITVs (perhaps as precursors), and that ITV/INTV bulbs were related to basolateral coated pits, which were generally larger than their apical counterparts, suggesting a functional difference consistent with involvement in basolateral exocytosis.

Common steps between FcRn-mediated transcytosis and other intracellular trafficking include transit through acidic vesicles and exocytosis/ligand release. Thus our studies of FcRn transcytosis in epithelial cells are also relevant to understanding FcRn's role in protecting IgG from degradation in endothelial cells[27] and other intracellular trafficking systems.

METHODS SUMMARY

Uptake of Au-Fc and Au-dextran

1.4nm monomaleimido-Nanogold was attached to reduced cysteine(s) in the rat Fc hinge, and sulfo-NHS-Nanogold was attached to dextran primary amines as described[7]. Labeled molecules were purified by FcRn affinity chromatography and/or gel filtration chromatography. For steady-state and immunolabeling experiments, 11- to 13-day suckling rats were fed 3×100μl of Au-Fc or Au-dextran (~3μM), after which the small intestine was harvested for chemical or cryofixation. For kinetic experiments, ligated intestines were incubated with 3μM Au-Fc (pulse experiments), followed by unlabeled Fc or IgG (pulse/chase experiments).

Gold enlargement procedures

Intestinal segments were chemically fixed, treated with GoldEnhance–EM 2113 (Nanoprobes, Inc.), and fixed/stained with OsO_4 and uranyl acetate as described[7]. Traditional pre-embedding enhancement protocols are incompatible with FSF, therefore we developed the methods for enlarging small gold clusters in the cold organic solvents used during FSF[7,10]. After HPF of intestinal segments, we used a three-step enlarging protocol involving silver enhancement to slightly enlarge (≤8nm) the Nanogold[10]; coating the silver shell with gold to make it impervious to osmium; and enlargement to 10-16nm using gold enhancement[7]. Samples were then treated with OsO_4 and uranyl acetate and warmed to room temperature.

Microscopy and 3D modeling

HPF/FSF or chemically-fixed samples were infiltrated with resin, polymerized, cut into 120-200nm sections, and examined using an FEI T12 transmission electron microscope operating at 120 kV. For tomography, dual axis tilt series were collected at 6500x from 120-200nm sections at 700nm underfocus. Tomograms were computed for each tilt axis using enlarged golds as alignment markers, and then aligned and combined to form a dual-axis tomogram using IMOD[28]. Unless otherwise indicated, tomographic slices were 1.6nm. Tomographic reconstructions were interpreted and modeled by manual segmentation using IMOD[28].

Immunolabeling

Immunolabeling was done on gold-enhanced intestinal samples using a modification of the Tokuyasu method for immunolabeling cryosections[29].

Supplementary Material

Refer to Web version on PubMed Central for supplementary material.

Acknowledgments

We thank David Mastronarde for advice about setting up SerialEM on the Caltech microscopes and 3D modeling; Christine Kivork for preparing Au-Fc and Au-dextran; Bill Tivol for assistance with electron microscopes; Marta Murphy for help with schematic figures; Mary Morphew for contributions to silver enhancement methods; Yonghong Nie, Alma Feuerabendt, Alex Kules, Carmen Luna, Kevin McKenzie, Robert Sander, and Leif Zinn-Bjorkman for segmenting tomograms; Jost Vielmetter for SPR studies of Au-Fc; and Frances Brodsky, Fred Maxfield, Sandra Schmid, and Devin Tesar for helpful discussions. This work was supported by the National Institutes of Health (2 R37 AI041239-06A1 to P.J.B. and RR000592 to J.R.M.), a Max Planck Research Award (P.J.B.), gifts from the Gordon and Betty Moore Foundation and the Agouron Institute to support electron microscopy at Caltech, and National University of Singapore AcRF startup funds (R-154-000-339-133 to W.H.).

References

1. Rodewald R, Kraehenbuhl J-P. Receptor-mediated transport of IgG. J. Cell Biol 1984;99:S159–S164.
2. Simister NE, Mostov KE. An Fc receptor structurally related to MHC class I antigens. Nature 1989;337:184–187. [PubMed: 2911353]
3. Rodewald R. Selective antibody transport in the proximal small intestine of the neonatal rat. J. Cell. Biol 1970;45:635–9193. [PubMed: 5459946]
4. Jones EA, Waldmann TA. The mechanism of intestinal uptake and transcellular transport of IgG in the neonatal rat. J. Clin. Invest 1972;51:2916. [PubMed: 5080417]
5. Rodewald R. Intestinal transport of antibodies in the newborn rat. J. Cell Biol 1973;58:189–211. [PubMed: 4726306]
6. Rodewald R. Distribution of immunoglobulin G receptors in the small intestine of the young rat. J. Cell Biol 1980;85:18–32. [PubMed: 7364873]
7. He W, et al. A Freeze Substitution Fixation-Based Gold Enlarging Technique for EM Studies of Endocytosed Nanogold-Labeled Molecules. J. Struct. Biol 2007;160:103–111. [PubMed: 17723309]
8. Benlounes N, et al. Intestinal transport and processing of immunoglobulin G in the neonatal and adult rat. Biol. Neonate 1995;67:254–263. [PubMed: 7647150]
9. McIntosh JR, Nicastro D, Mastronarde DN. New views of cells in 3D: an introduction to electron tomography. Trends Cell Biol 2005;15:43–51. [PubMed: 15653077]
10. Morphew M, He W, Bjorkman PJ, McIntosh JR. Silver enhancement of nanogold particles during freeze substitution fixation for electron microscopy. J Microscopy 2008;230:263–267.
11. Hull BE, Staehelin LA. The terminal web. A reevaluation of its structure and function. J. Cell Biol 1979;81:67–82. [PubMed: 573268]
12. Schwartz SL, Cao C, Pylypenko O, Rak A, Wandinger-Ness A. Rab GTPases at a glance. J Cell Sci 2007;120:3905–10. [PubMed: 17989088]
13. Stoorvogel W, Oorschot V, Geuze HJ. A novel class of clathrin-coated vesicles budding from endosomes. J. Cell Biol 1996;132:21–33. [PubMed: 8567724]
14. McCarthy KM, Yoong Y, Simister NE. Bidirectional transcytosis of IgG by the rat neonatal Fc receptor expressed in a rat kidney cell line: a system to study protein transport across epithelia. J Cell Sci 2000;113:1277–85. [PubMed: 10704378]
15. Murk JLAN, et al. Endosomal compartmentalization in three dimensions: Implications for membrane fusion. Proc. Natl. Acad. Sci. USA 2003;100:13332–13337. [PubMed: 14597718]
16. Kleijmeer M, et al. Reorganization of multivesicular bodies regulates MHC class II antigen presentation by dendritic cells. J. Cell Biol 2001;155:53–63. [PubMed: 11581285]

17. Mari M, et al. SNX1 Defines an Early Endosomal Recycling Exit for Sortilin and Mannose 6-Phosphate Receptors. Traffic 2008;9:380–93. [PubMed: 18088323]

18. Altstiel L, Branton D. Fusion of coated vesicles with lysosomes: measurement with a fluorescence assay. Cell 1983;32:921–9. [PubMed: 6131746]

19. Brodsky FM, Chen CY, Knuehl C, Towler MC, Wakeham DE. Biological basket weaving: formation and function of clathrin-coated vesicles. Annu Rev Cell Dev Biol 2001;17:517–68. [PubMed: 11687498]

20. Conner SD, Schmid SL. Regulated portals of entry into the cell. Nature 2003;422:37–44. [PubMed: 12621426]

21. Bonifacino JS, Glick BS. The mechanisms of vesicle budding and fusion. Cell 2004;116:153–66. [PubMed: 14744428]

22. Greene LE, Eisenberg E. Dissociation of clathrin from coated vesicles by the uncoating ATPase. J Biol Chem 1990;265:6682–7. [PubMed: 1969864]

23. Fesce R, Grohovaz F, Valtorta F, Meldolesi J. Neurotransmitter release: fusion or 'kiss-and-run'? Trends Cell Biol 1994;4:1–4. [PubMed: 14731821]

24. Ober RJ, Martinez C, Lai X, Zhou J, Ward ES. Exocytosis of IgG as mediated by the receptor, FcRn: an analysis at the single-molecule level. Proc Natl Acad Sci U S A 2004;101:11076–81. [PubMed: 15258288]

25. Sokac AM, Bement WM. Kiss-and-coat and compartment mixing: coupling exocytosis to signal generation and local actin assembly. Mol Biol Cell 2006;17:1495–502. [PubMed: 16436510]

26. Granseth B, Odermatt B, Royle SJ, Lagnado L. Clathrin-mediated endocytosis is the dominant mechanism of vesicle retrieval at hippocampal synapses. Neuron 2006;51:773–86. [PubMed: 16982422]

27. Ghetie V, Ward ES. Multiple roles for the major histocompatibility complex class I-related FcRn. Annu. Rev. Immunol 2000;18:739–766. [PubMed: 10837074]

28. Mastronarde DN. Dual-axis tomography: an approach with alignment methods that preserve resolution. J Struct Biol 1997;120:343–52. [PubMed: 9441937]

29. Ladinsky MS, Howell KE. Electron tomography of immunolabeled cryosections. Methods Cell Biol 2007;79:543–58. [PubMed: 17327173]

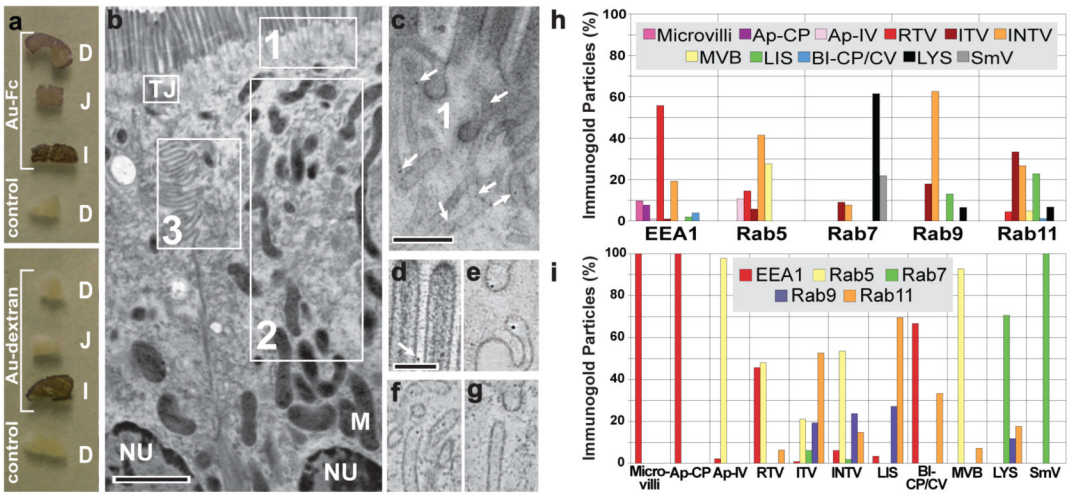

Figure 1. Au-Fc uptake in intestinal cells

Bar=2μm (b); 300nm (c); 200nm (d-g). (a) Chemically-fixed/gold-enhanced intestinal samples from the duodenum (D), jejunum (J) and ileum (I) of Au-Fc-fed, Au-dextran-fed, and control rats (Supplementary Fig.S7 shows corresponding projections). (b-c) Projections of jejunal sections showing Regions 1-3 (b; 180nm section) or 1 (c; 150nm section). (See also Supplementary Fig.S3-S6.) "TJ": tight junction; "NU": nucleus; "M": mitochondrion. White arrows: Au-Fc in RTVs. (d-g) Tomograhic slices showing Au-Fc in Region 1 on (d) microvilli, (e) coated pit and apical irregular vesicle, (f) RTVs, apical irregular vesicles, (g) RTV proximal to a coated pit. (h-i) Histograms constructed using the immunolabeling data in Supplementary Table S2. Ap-CP: apical coated pits/coated vesicles; Ap-IV: apical irregular vesicles; Bl-CP/CV: basolateral coated pits/coated vesicles; LYS: lysosomes; SmV: 30-40nm vesicles related to lysosomes. (h) Percent of each marker found in each structure. (i) Percent of each structure that was positive for each marker.

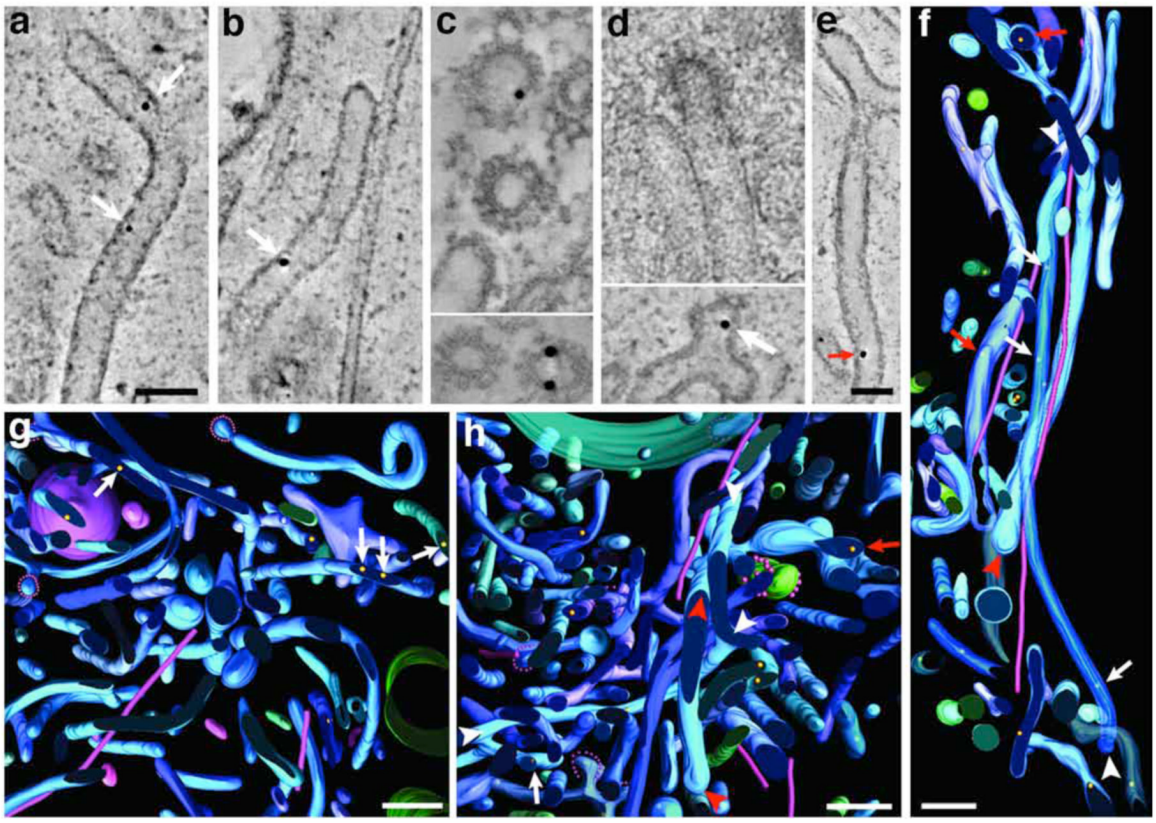

Figure 2. Gold-containing tubular vesicles from jejunal Regions 1-2

Bar=100nm (a-d,e) or 200nm (f-h). c is chemically-fixed; others are HPF/FSF. White arrowheads: RTVs; white arrows: Au-Fc in RTVs; red arrowheads: ITVs; red arrows: Au-Fc in ITVs. Colours for segmented models in all figures and movies: Tubular and irregular vesicles (blue shades); microtubules (pink straws); lysosomes (violet); rough ER (green with scarlet ribosomes); mitochondria (bright green); LIS membranes (purple and blue); clathrin coats (small red spheres around blue vesicles/ buds); Au-Fc (gold spheres). (a-b) RTVs (associated with a microtubule in b). (c) Small (<70nm) coated vesicles. (d) Small (<70nm) coated buds. (e) ITV. (f-h) Models showing the cellular contexts of tubular vesicles (corresponding to Supplementary Movies 2-3; Supplementary Fig.S4b,S10a-b;S11a-b).

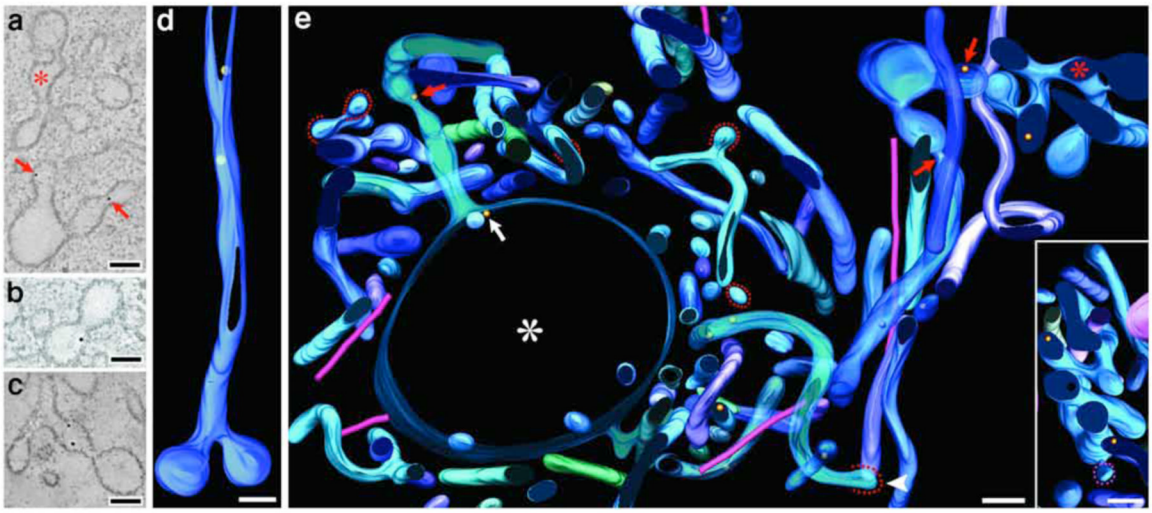

Figure 3. Gold-containing irregular vesicles in jejunal Regions 2-3

Bar=100nm. Tomographic slices (a-c) and models (d-e; coloured as in Fig. 2). (a-c) INTVs (asterisk in a). ITV (red arrows in a). (d-e) Segmented models, coloured as in Fig.2. (d) ITV. (e) The cellular context of irregular vesicles (see Supplementary Movie 4), including a MVB (white asterisk) with Au-Fc on the main membrane (white arrow) and in a tubular protrusion (red arrow). Top right of e corresponds to a (see red asterisks and arrows). Inset in e shows entangled irregular vesicles.

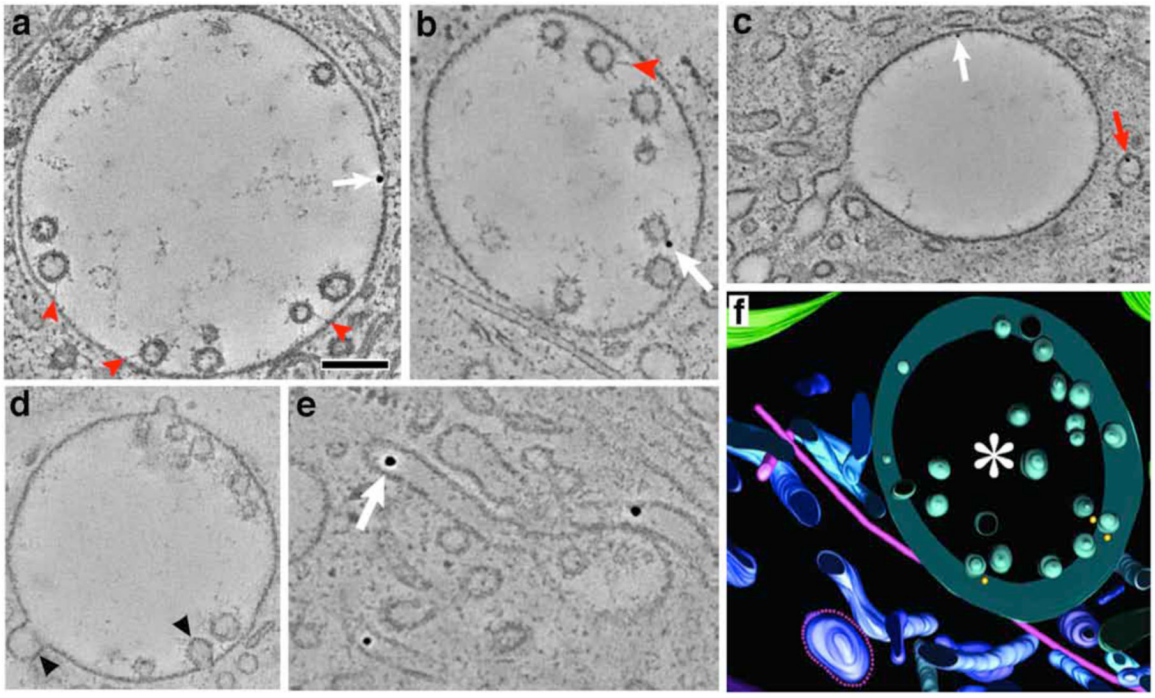

Figure 4. Gold-containing MVBs in jejunal cells

Bar=200nm. Tomographic slices (a-e) and model (f; coloured as in Fig.2). White arrows: Au-Fc on MVB main and inner vesicle membranes; red arrow: Au-Fc in a spherical vesicle; red arrowheads: fibrous extensions connecting inner vesicles with each other or the main membrane; black arrowheads: MVB invagination or protrusion. (a-e) Inner vesicles, invaginations and outward projections in MVBs. (f) Model showing the MVB (white asterisk) in b (corresponding projection and larger model in Supplementary Fig.S10c,S11c).

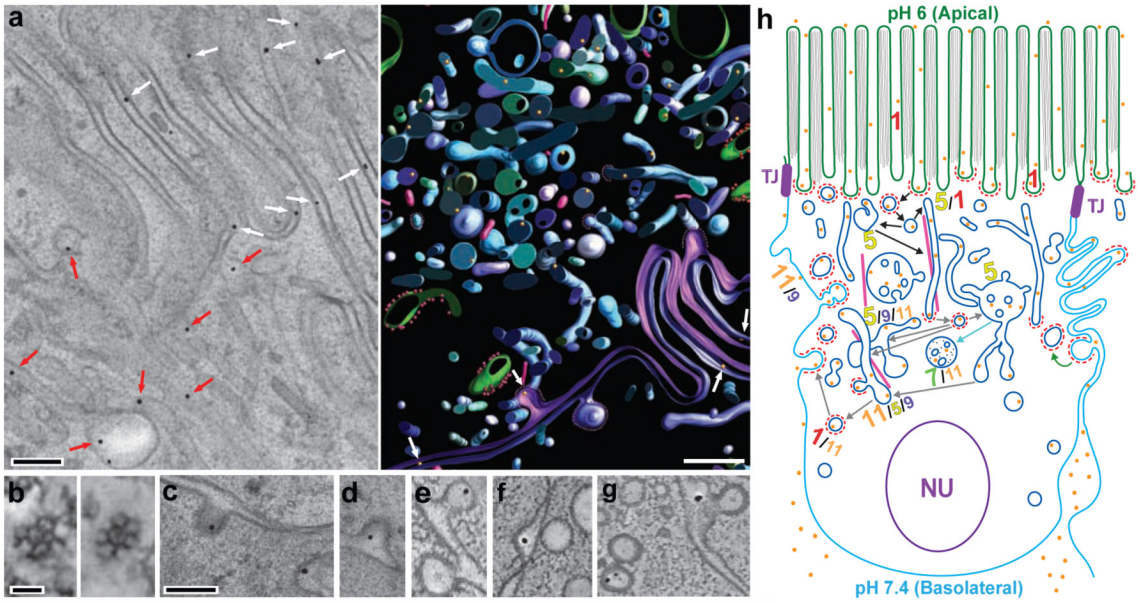

Figure 5. Jejunal LIS and schematic pathways

Bar =200nm (a,c-g) or 50nm (b). White arrows: Au-Fc in LIS; red arrows: Au-Fc in irregular vesicles. (a) LIS and vicinity as projection (left) and segmented model (right; coloured as in Fig.2). (b) Hexagonal (left) and heptagonal (right) clathrin lattices (chemically-fixed samples). (c-g) Au-Fc in coated pits. (c and d are projections.) (h) Schematic of FcRn-mediated transcytosis. "TJ": tight junctions; "NU": nucleus; green: apical membrane; cyan: basolateral membrane; red dashes: clathrin; pink straws: microtubules; gold spheres: Au-Fc; black arrows: early trafficking steps; gray arrows: later trafficking steps; green arrow: endocytosis of FcRn-containing coated pit after ligand release; cyan arrow: excess Au-Fc transferred to late endosome (rarely observed). Multiple arrows indicate parallel pathways. Vesicles shown using schematic models (Supplementary Fig.S8) at a lower density and larger size than observed. Numbers beside schematic vesicles refer to endosomal markers (1=EEA1, 5=Rab5, 7=Rab7, 9=Rab9, 11=Rab11); the font size reflects relative amounts of label in each type of compartment (see Fig.1i).